Critical role of boreal summer North Pacific subtropical highs in ENSO transition

Kyung-Sook Yun, Kyung-Ja Ha, Sang-Wook Yeh, Bin Wang & Baoqiang Xiang

Climate Dynamics
Observational, Theoretical and Computational Research on the Climate System

ISSN 0930-7575

Clim Dyn
DOI 10.1007/s00382-014-2193-6

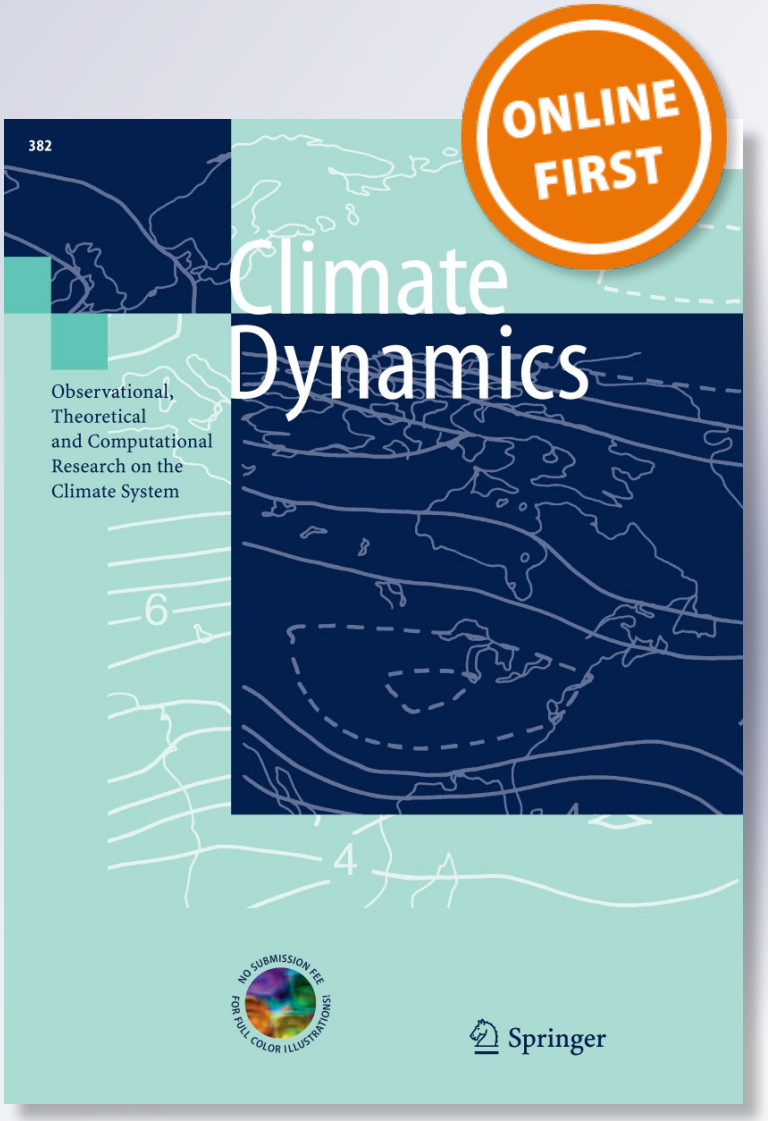

Springer

Clim Dyn
DOI 10.1007/s00382-014-2193-6

Critical role of boreal summer North Pacific subtropical highs in ENSO transition

Kyung-Sook Yun · Kyung-Ja Ha · Sang-Wook Yeh · Bin Wang · Baoqiang Xiang

Received: 4 December 2013 / Accepted: 20 May 2014

Abstract The quasi-biennial (QB)-type El Niño-Southern Oscillation (ENSO), showing a fast phase transition from El Niño to La Niña, is closely related to the variability of the North Pacific subtropical high (NPSH) and western North Pacific subtropical high (WNPSH) during summer. Here, we show that the NPSH plays a key role in the fast ENSO transition. The QB-type ENSO is associated with both strengthened WNPSH and NPSH during the boreal summer. By contrast, the low-frequency-type ENSO, which occurs in a typical period of 3–7 years, displays an enhanced WNPSH but weakened NPSH. The stronger El Niño tends to generate a more intensified WNPSH from spring to summer, leading to the initial decay of El Niño via the modulation of easterly wind in the western Pacific. On the contrary, the NPSH has greater linkage with the decaying El Niño process after the boreal summer. Therefore, the coupled pattern of WNPSH–NPSH is important in changing ENSO phase from El Niño to La Niña. The NPSH causes sea surface temperature cooling over the subtropical Northeastern Pacific. The resultant subtropical cooling induces anomalous anticyclone west of the reduced heating, which generates the strengthening of trade winds south of the anticyclone. Consequently, this process contributes to tropical central Pacific cooling and the rapid transition of El Niño to La Niña. This study hints that the QB-type ENSO could be significantly linked to a tropics-midlatitudes coupled system such as an in-phase pattern between WNPSH and NPSH. The results are useful for improvement of ENSO prediction.

Keywords Fast El Niño transition · QB-type ENSO · Western North Pacific subtropical high · North Pacific subtropical high · Tropics-midlatitudes coupled system

K.-S. Yun · K.-J. Ha (✉)
Division of Earth Environmental System, Department of Atmospheric Sciences, College of Natural Science, Pusan National University, Busan, Korea
e-mail: kjha@pusan.ac.kr

S.-W. Yeh
Department of Marine Sciences and Convergent Technology, Hanyang University, ERICA, Ansan, Korea

B. Wang
Department of Meteorology, School of Ocean and Earth Science and Technology, University of Hawaii at Manoa, Honolulu, HI, USA

B. Xiang
NOAA/Geophysical Fluid Dynamics Laboratory, Princeton, NJ, USA

B. Xiang
University Corporation for Atmospheric Research, Boulder, CO, USA

1 Introduction

El Niño-Southern Oscillation (ENSO) is one of the most important variabilities of an atmosphere–ocean coupled system and has worldwide implications over global weather and climates. The major variability of ENSO can be explained in terms of two dominant frequencies (Barnett 1991). One is the quasi-biennial (QB)-type ENSO with a period of 2–3 years, and the other is the low-frequency (LF)-type ENSO (or quasi-quadrennial-type) with a typical period of 3–7 years. The distinct time scales of ENSO have fundamental differences in their seasonal evolutions and dynamics (Kim and Kim 2002; Wang and An 2005; Bejarano and Jin 2008). For example, Barnett (1991) has shown that the QB-type ENSO is associated with a

Published online: 30 May 2014

quasi-progressive wave, whereas the LF-type ENSO appears to be related to a standing wave. Bejarano and Jin (2008) have reported that the phase transition of the QB-type ENSO is modulated by anomalous advection of sea surface temperature (SST) by equatorial zonal current anomalies, whereas that of the LF-type ENSO is determined by slow oceanic dynamic adjustment of equatorial heat content. The two different types of ENSO determine whether El Niño events persist or decay rapidly. In particular, the QB-type ENSO is closely related to the fast termination of ENSO through a strong oceanic Kelvin and Rossby wave response (Kim and Kim 2002). The main objective of the present study is to examine the process that leads to the abrupt decaying of El Niño through the transition to La Niña, which is associated with QB-type ENSO.

Previous studies have suggested that the South Asian monsoon plays an important role in the modulation of the QB-type ENSO, which is associated with tropospheric biennial oscillation (TBO) as an intrinsic atmosphere–ocean–land coupled mode over the tropical Indo-Pacific region (Yasunari 1990; Meehl 1997; Wu and Kirtman 2004). In relation to the early decaying nature of the QB-type ENSO, anomalous wind forcing in the western North Pacific (WNP), which is affected by both anomalous Indian Ocean warming and the local air–sea interaction (Kim and Lau 2001; Kug and Kang 2006; Chen et al. 2012), holds the key for the transition from El Niño to La Niña via the thermocline adjustment and the response of equatorial Kelvin waves (Weisberg and Wang 1997; Wang et al. 1999). Moreover, a biennial signal has been revealed in the East Asian summer monsoon (EASM)-ENSO relationship (Shen and Lau 1995; Chang et al. 2000; Yun et al. 2009): A strong EASM is preceded by preceding El Niño, and this signal undergoes changes from the monsoon summer to the following winter, leading to a La Niña. These studies on the EASM–ENSO relationship indicate several potential links between summer extratropical circulation and the QB-type ENSO.

On the other hand, several recent studies have reported that extratropical circulation can trigger ENSO (Vimont et al. 2003; Liu and Yang 2003; Yu et al. 2010; Yu and Kim 2011). For example, Liu and Yang (2003) have explained the extratropical control on tropical SST in terms of the atmospheric bridge of the Hadley circulation ($\sim$70 %) and the oceanic tunnel of thermocline subduction ($\sim$30 %). Vimont et al. (2003) have shown that the preceding winter North Pacific oscillation (NPO) affects the following winter tropical SST change via the seasonal footprint mechanism. However, the exact role of summer extratropical circulation on the abrupt decaying of El Niño has not been fully investigated yet.

Most such studies of North Pacific have focused on the winter season because most climate variabilities such as ENSO and NPO tend to peak in the boreal winter. Meanwhile, the relationship between ENSO and summer extratropical circulation has been mainly highlighted in the western North Pacific subtropical high (WNPSH) (e.g., Wang et al. 2000; Chang et al. 2000; Li et al. 2007; Yun et al. 2011; Chen et al. 2012). However, magnitude of the North Pacific subtropical high (NPSH) is most prominent during the boreal summer; summertime atmospheric circulation in the extratropical North Pacific is dominated by the interplay between the NPSH and WNPSH (Yun et al. 2013). In particular, the wind variability in the WNP is strongly controlled by boreal summer subtropical highs. Although several studies (e.g., Rodwell and Hoskins 2001; Lau et al. 2004) have investigated the role of the North Pacific on climate during the summer season, the possible connection of subtropical highs and the termination of El Niño has yet to be addressed. In the present study, we aim to answer the fundamental questions of how the extratropical circulations regulate the rapid termination of El Niño and of which extratropical circulation component affects the decaying process. Major emphasis has been placed on the distinct roles of summer WNPSH and NPSH in determining the rapid El Niño decay by comparing the QB- and LF-type ENSO.

The remainder of this paper is organized as follows. Section 2 presents the data, methodology such as the definitions of QB and LF-type ENSO, and the description of the coupled ocean–atmosphere model. Section 3 shows extratropical responses in relation to ENSO transition. Section 4 illustrates the roles of the NPSH and WNPSH on the ENSO transition based on observation and numerical modelling. Section 5 discusses and summarizes the results.

2 Data, method, and model

2.1 Data

The present study used monthly-mean atmospheric variables obtained from the National Centers for Environmental Prediction–Department of Energy (NCEP–DOE) Reanalysis version 2 (NCEP2; Kanamitsu et al. 2002) for the period 1979–2010 and from NCEP–National Center for Atmospheric Research (NCAR) (NCEP; Kalnay et al. 1996) for the period 1958–2010. To rule out the effects of interdecadal change on ENSO after the late 1970s, the period displayed here used NCEP2 data from 1979 to 2010, however all analyses were also performed during 1958–2010 years with NCEP data. The main results from these two data types and periods were nearly consistent (Figure not shown). Surface wind stress data obtained from Simple Ocean Data Assimilation (SODA) 2.0.2-4 Reanalysis (Carton and Giese 2008) for the period 1958–2007 was

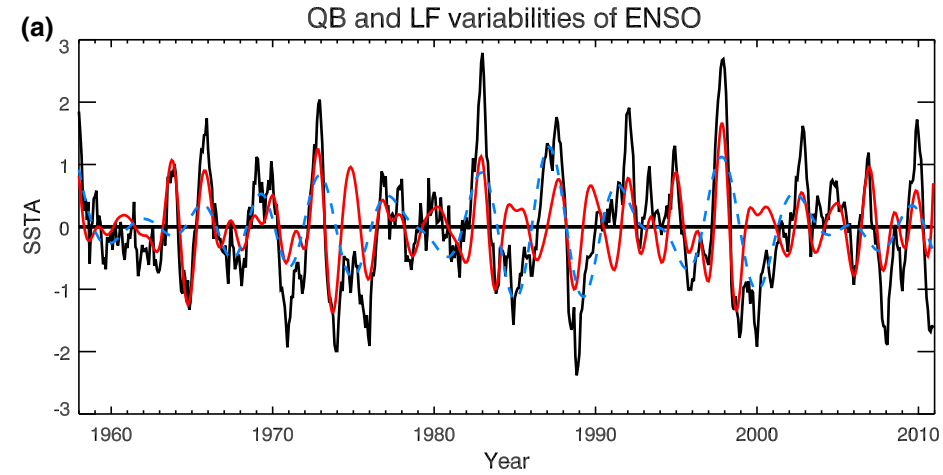

(c)

ENSO type	Years
QB-type ENSO	63/64, 69/70, 72/73, 82/83, 87/88, 94/95, 97/98, 06/07, and 09/10
LF-type ENSO	57/58, 65/66, 68/69, 76/77, 86/87, 91/92, and 02/03

Fig. 1 **a** Monthly timeseries of Niño3.4 (*black solid line*), QB (*red solid line*), and LF (*blue dashed line*) filtered Niño3.4 anomaly indexes (QB and LF variabilities) from 1958 to 2010. **b** Temporal change of Niño3.4 anomaly index averaged for total El Niño years, QB-type ENSO years, and LF-type ENSO years. **c** The selected nine QB-type and seven LF-type El Niño years

also used. The rainfall data were obtained from the Global Precipitation Climatology Project (GPCP) version 2.2 combined precipitation dataset (Adler et al. 2003). This study also used SST obtained from Met Office Hadley Centre Sea Ice and Sea Surface Temperature version 1.1 (HadISST1.1) (Rayner et al. 2003), available from 1870 to the present.

2.2 Definition of QB and LF-type ENSO

For identifying ENSO years, the monthly Niño3.4 index [5°S–5°N, 170°W–120°W] derived from *Climate Prediction Center (CPC)–National Oceanic and Atmospheric Administration* (NOAA) data was used. QB- and LF-types ENSO were roughly defined by two methodologies. A band-pass filter was first applied to separate the monthly Niño3.4 index into QB (2–3 years) and LF (3–7 years) variability. The filtering period was given at the half-power points at 16 and 36 months for QB and 42 and 86 months for LF, based on the study of Li and Zhang (2002). The QB and LF-band filtered Niño3.4 indices are referred to as QB and LF variability of ENSO. The variability of QB is not significantly correlated with that of LF during the El Niño winter (correlation coefficient $r \sim 0.17$). The monthly timeseries of original, QB-, and LF-component Niño3.4 anomalies are displayed in Fig. 1a. In the second methodology, the cases of QB- and LF-type ENSO years were selected from the long-term unfiltered data of 1958–2010. The QB-type ENSO cases were identified as years in which the preceding winter (December-to-February(0), DJF(0)) El Niño is changed into La Niña in the following summer (July-to-September(0), JAS(0)). Years in which the SST difference between the preceding winter and ensuing summer is greater than 2.0 °C (i.e., 1982/1983) were also defined as QB-type ENSO cases. On the other contrary, LF-type ENSO cases were defined as years when the preceding winter El Niño is sustained until the ensuing summer season with Niño3.4 anomalies greater than 0 °C. Here, El Niño (La Niña) is defined in terms of a normalized Niño3.4 index greater (less) than 0.5 (−0.5). The QB-type ENSO reveals much rapider termination of warming than that observed in the LF-type ENSO cases; this difference

initiates in the following spring and is manifest after the summer monsoon season (Fig. 1b). The selected ENSO years are presented in Fig. 1c.

2.3 Coupled model: POP-OASIS-ECHAM model

The coupled model used in this study is POP-OASIS-ECHAM model (POEM) developed by Xiang et al. (2012), in which ECHAM4.6 (atmosphere component; Roeckner et al. 1996) is coupled to the Parallel Ocean Program (POP, v2.0; Smith et al. 1992) ocean model through the Ocean Atmosphere Sea Ice Soil (OASIS 3.0; Valcke et al., 2000) coupling software package. The atmospheric model has T42 horizontal spectral truncation (128 × 64) with 19 vertical layers, whereas the ocean model is calculated on a 100 × 116 horizontal grid with 25 vertical layers. The fully coupled region is confined between 60°S and 60°N, outside of which the atmospheric model is specified as the climatological monthly mean SSTs and sea ices. The atmosphere model provides daily mean surface wind stress, heat and fresh water fluxes to the ocean model and the ocean model sends daily mean SST and ocean surface currents back to the atmosphere model. The coupling frequency is one day but with an idealized solar radiation diurnal cycle (Danabasoglu et al. 2006). The model is a useful tool for examining basic processes in the coupled climate system; a detailed description of POEM is presented in Xiang et al. (2012).

3 Different extratropical responses to ENSO transition

The QB- and LF-type ENSOs have different ENSO cycles (Barnett 1991). The former is characterized by an abrupt termination of an El Niño event that evolves into a La Niña event after the summer monsoon season. Because of a significant association between unfiltered Niño3.4 and QB (or LF) filtered indices during the El Niño winter ($r \sim 0.71$ for both of QB and LF with Niño3.4), there is a considerable overlap between QB and LF-regressed winter patterns, which makes it difficult to separate the QB and LF ENSO winter patterns using the simple regression analysis. To explore the circulation variability, therefore, we have shown the composite of SST and low-level (850 hPa) geopotential height (Z850) anomalies for the QB- and LF-type ENSO years (Fig. 2). The QB- and LF-type ENSO years are categorized according to the second methodology on ENSO type (see Sect. 2.2 and Fig. 1c): after 1979, six QB-type ENSO winters are 1982/1983, 1987/1988, 1994/1995, 1997/1998, 2006/2007, and 2009/2010, and three LF-type ENSO winters are 1986/1987, 1991/1992, and 2002/2003. During the El Niño winter, the QB and LF reveal an ENSO—related pattern such as eastern Pacific warming, western Pacific cooling, and Indian Ocean warming with zonal pressure differences between the eastern and western Pacific. However, the QB-type ENSO shows a warmer Indian Ocean SST anomaly than the LF-type ENSO. Meanwhile, the LF-type ENSO exhibits a cooler western Pacific SST anomaly and central Pacific warming center than the QB-type ENSO. The decay of El Niño is initiated in the spring (March to May; MAM(0)) and this cooling tendency is stronger in QB than that in LF (Fig. 2c, d). Prominent differences between QB and LF begin to occur in the following summer season (JJA(0)). The abrupt phase change from El Niño into La Niña is presented in the QB summer (Fig. 2e), while sustained eastern Pacific warming occurs in the LF summer (Fig. 2f). According to the well-known impact of ENSO on summer extratropical circulation (e.g., Wang et al. 2000; Yun et al. 2013), a significant anomalous WNPSH appears in both the QB- and LF-type ENSO years during JJA(0). Of particular interest is that the WNPSH coexists with the strengthened NPSH for the QB-type ENSO summer, in contrast to a weakened NPSH occurring in the LF-type ENSO summer. The enhanced summertime NPSH during the QB-type ENSO is consistent with that reported by Yun et al. (2009).

To focus on the change in summer extratropical circulation, the regressed fields of summer Z850 and surface wind stress anomalies against the QB- and LF-filtered variability of ENSO are displayed in Fig. 3, together with the composite fields for the QB- and LF-type ENSO years, respectively. The striking difference in low-level circulation between QB and LF variabilities is shown in consistent response with the composite pattern for the QB- and LF-type ENSO years. As an important signal of QB-type ENSO, the in-phase relationship between WNPSH and NPSH appears in the boreal summer, which differs distinctly from the out-of-phase relationship for the LF-type ENSO. Note that easterly wind stress anomalies are most evident in the western and central Pacific along the southern flank of the anomalously strong WNPSH for the QB-type ENSO cases, while the easterly wind anomalies are relatively weaker for the LF-type ENSO cases. The western Pacific easterly wind forcing may contribute to the rapid termination of El Niño by generating an upwelling of oceanic Kelvin waves (Wang et al. 1999; Kim and Lau 2001; Kug and Kang 2006). Although conspicuous Z850 variability shows in its western edge of the NPSH for these two types of ENSO, the summertime NPSH reveals more prominent differences relative to QB- and LF-type ENSO. In detail, the negative NPSH is situated in LF-type ENSO cases, whereas the anomalous high NPSH exists in QB-type ENSO cases, which implies that the summertime coupled pattern of NPSH–WNPSH plays a vital role in maintaining the abrupt termination of El Niño.

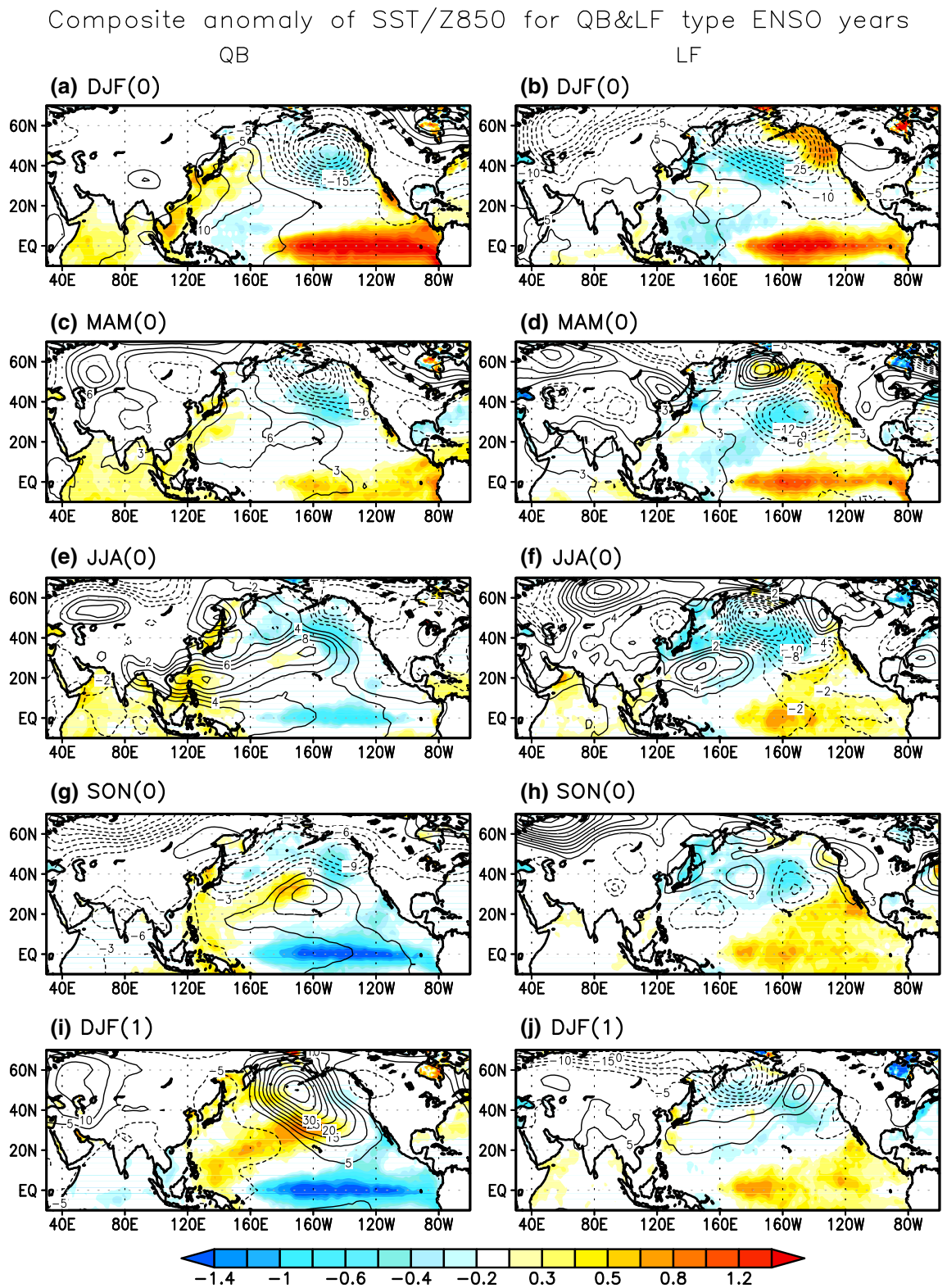

Fig. 2 Seasonal sequence of composite anomaly of SST (*shading*) and geopotential height at 850 hPa (*contour*) for (*left*) QB- and (*right*) LF-type ENSO years during 1979–2010

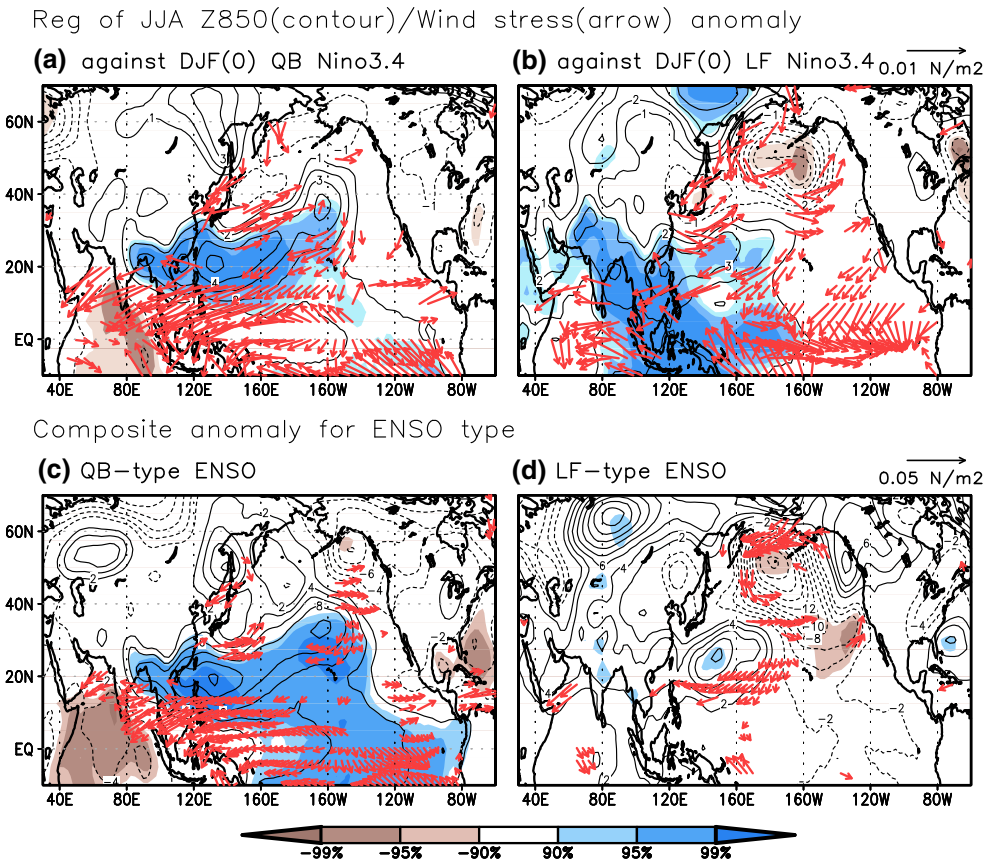

Fig. 3 **a**–**b** Regressed field of the JJA geopotential height at 850 hPa (*contour*) and surface wind stress (*arrow*) anomaly against the preceding winter **a** QB and **b** LF Niño3.4 index during 1979–2010. **c**–**d** Composite field of the JJA geopotential height at 850 hPa (*contour*) and surface wind stress (*arrow*) anomaly for **c** QB and **d** LF-type ENSO year during 1979–2010. The *shading* indicates the significant geopotential height anomaly above the 90 % confidence level

4 Role of North Pacific subtropical highs on ENSO transition

The QB- and LF-type ENSO years reveal primary differences in extratropical summer circulation, which is characterized by the WNPSH and NPSH. To examine the relationship between the subtropical highs and ENSO transition, the NPSH and WNPSH are defined as the area-averaged sea level pressure (SLP) anomalies over [30°N–40°N, 170°W–140°W] and [15°N–25°N, 110°E–150°E], respectively (Yun et al. 2013). Figure 4 displays the longitude-time section of lead-lag regression of SST and 850 hPa zonal wind anomaly averaged over the equatorial band (5°S–5°N) against the JJA NPSH and WNPSH indices during 1979–2010. Here, the reference month is July, and the regression in the lag 0 month represents the relationship between July SST (or zonal wind) and JJA highs. For example, a negative 6-month time lag indicates that the preceding winter El Niño leads the summer subtropical highs. As the result, the WNPSH is well-linked to the biennial relationship with ENSO: a strong WNPSH is preceded by the preceding winter El Niño, which is changed from summer to the following winter, leading to a La Niña. The NPSH, meanwhile, is more significantly connected with the following winter La Niña than with the preceding winter El Niño. Such distinction suggests that the NPSH is more tightly linked to the El Niño decaying process than the WNPSH is. The regressed zonal wind anomaly also represents this lead-lag relationship between ENSO and subtropical highs (Fig. 4c, d). The easterly wind anomaly in the western Pacific, which plays a key role in El Niño decay, is definitely correlated with the both WNPSH and NPSH after the concurrent summer. During the boreal summer (i.e., from −1 to 1 lag month), the NPSH-related easterly wind anomaly is manifested in the central Pacific over [160°E–160°W], which contrasts with the WNPSH-related wind anomaly centered in the western Pacific over [120°E–160°E] (Fig. 4e). This result is indicative of the significant impact of the summertime NPSH on ENSO decay, in contrast to that of the WNPSH.

However, it cannot be ruled out that a strong El Niño event tends to generate a strong WNPSH that lasts from

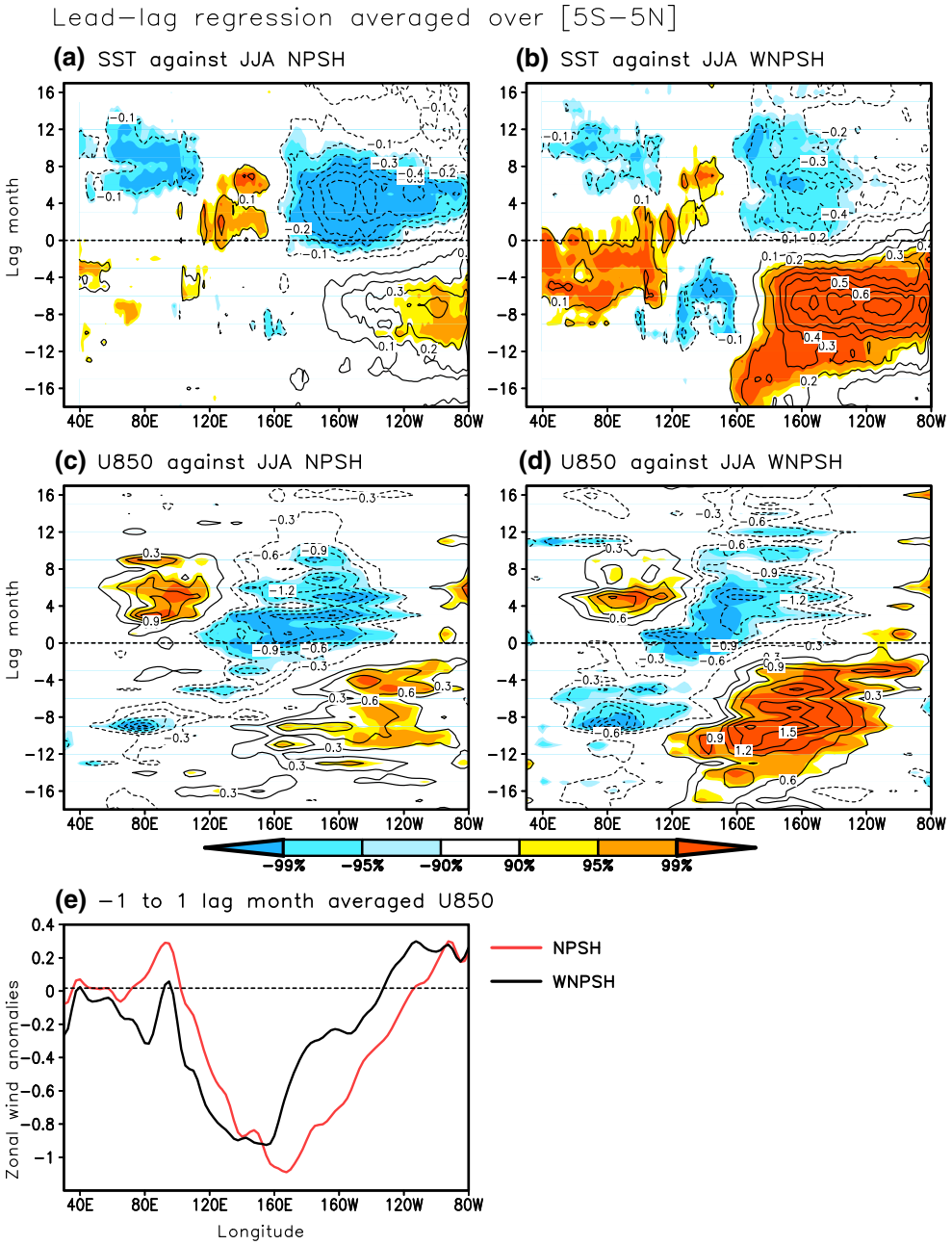

Fig. 4 **a–b** Lag-lead regression of SST anomaly averaged over the equatorial area [5°S–5°N] against the JJA **a** North Pacific subtropical high (NPSH) and **b** western North Pacific subtropical high (WNPSH) during 1979–2010. **c–d** Same as **a–b**, but for 850 hPa zonal wind anomaly. The *shading* indicates the significant anomaly above the 90 % confidence level. **e** Zonal structure of regressed 850 hPa zonal wind anomaly against NPSH (*red line*) and WNPSH (*black line*) averaged during −1 to 1 lag month

spring to summer, providing the persistent easterly wind anomaly in the equatorial western Pacific (Wang and Li 2004; Li et al. 2007; Liu and Xue 2010a). As shown in Fig. 1, the significant El Niño deterioration and WNPSH begin to develop in the boreal spring and persists into summer. Wang and Li (2004) have demonstrated that the springtime WNPSH contributes significantly to the development of upwelling oceanic Kelvin waves and the resultant initiation of the El Niño demise. To review the relationship between the springtime WNPSH and ENSO intensity, we have presented in Fig. 5a a scatter diagram of wintertime Niño3.4 index and springtime WNPSH during a longer period from 1958 to 2010. Here, the events with the Niño3.4 index averaged in the El Niño winter (DJF) being greater than 1.5 standard deviation were classified as strong El Niño events, and the rest were classified as moderate El

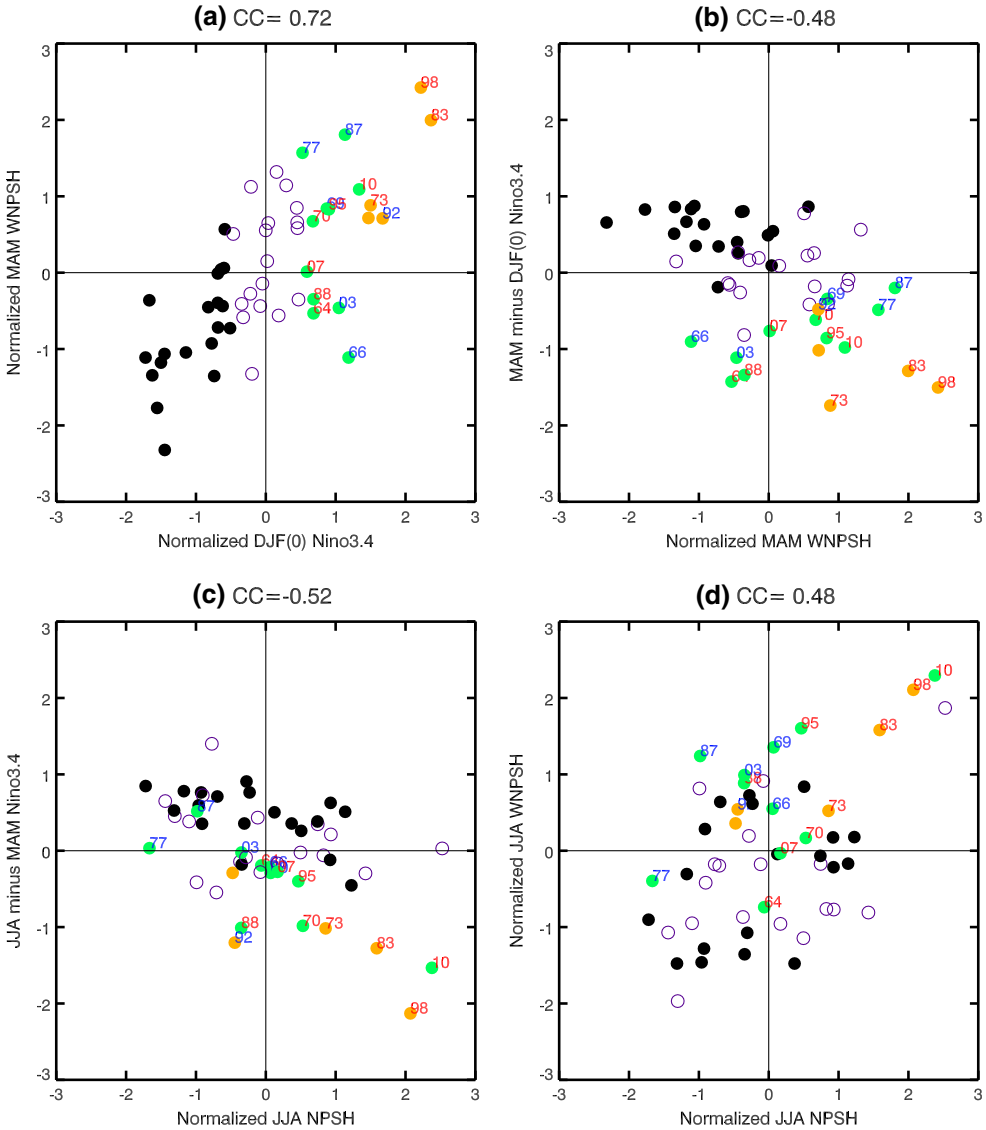

Fig. 5 **a** Scatter diagram of normalized DJF(0) Niño3.4 SST anomaly (x-axis) versus normalized MAM WNPSH (y-axis) during 53 years from 1958 to 2010. **b–d** Same as **a**, but for **b** normalized MAM WNPSH versus difference of MAM minus DJF(0) Niño3.4 SST, **c** normalized JJA NPSH versus difference of JJA minus MAM Niño3.4 SST, and **d** normalized JJA NPSH versus JJA WNPSH. The *black closed circles* indicate the La Niña years, while the *green* and *yellow closed circles* indicate moderate and strong El Niño years, respectively. The *open circles* denote the normal years. The *red color* two-digit numbers (e.g., 98) represent the QB-type ENSO years (e.g., 1997/1998 year), while the *blue color* two-digit numbers show the LF-type ENSO years

Niño events. This criterion identified 5 strong El Niño events and 11 moderate events, represented in the figure by orange and green colors, respectively. In addition to the ENSO intensity, the QB- and LF-type ENSO years are displayed in the digital numbers colored red and blue, respectively. For example, "98" indicates the 1997/1998 winter El Niño event defined as a QB-type ENSO. As expected, a stronger El Niño excites a stronger springtime WNPSH ($r \sim 0.72$).

In fact, a stronger springtime WNPSH is associated with a greater cold SST tendency during the boreal spring (i.e., spring minus winter Niño3.4 index) ($r \sim -0.48$), which is shown in Fig. 5b. This result suggests that the anomalous WNPSH is responsible for the initiation of El Niño decay during the boreal spring. On the contrary, during the boreal summer, the stronger NPSH is related to the greater cold SST tendency ($r \sim -0.52$), which is shown in Fig. 5c. Despite of the strong summer WNPSH anomaly, some El Niño years (i.e., 1986/1987 and 2002/2003) have a relatively weak cold SST tendency, which coincides with the weakened NPSH. In addition, some El Niño years (i.e., 1969/1970, 2009/2010) show a stronger cold tendency during summer than that during spring, which coexists with the strengthened summer NPSH. Note that the strong El Niño events do not always coincide with the QB-type ENSO events, which indicates that the summertime NPSH is significantly related to the El Niño transition into La Niña, leading to the QB-type ENSO. As a result, the coupled pattern of strong NPSH and WNPSH appears in the QB-type ENSO, while the out-of-phase pattern of weak NPSH and strong WNPSH is seen in the LF-type ENSO (Fig. 5d). It is evident that the NPSH variability during the boreal summer is significantly linked to ENSO type. Eventually, the WNPSH is related to the initiation of

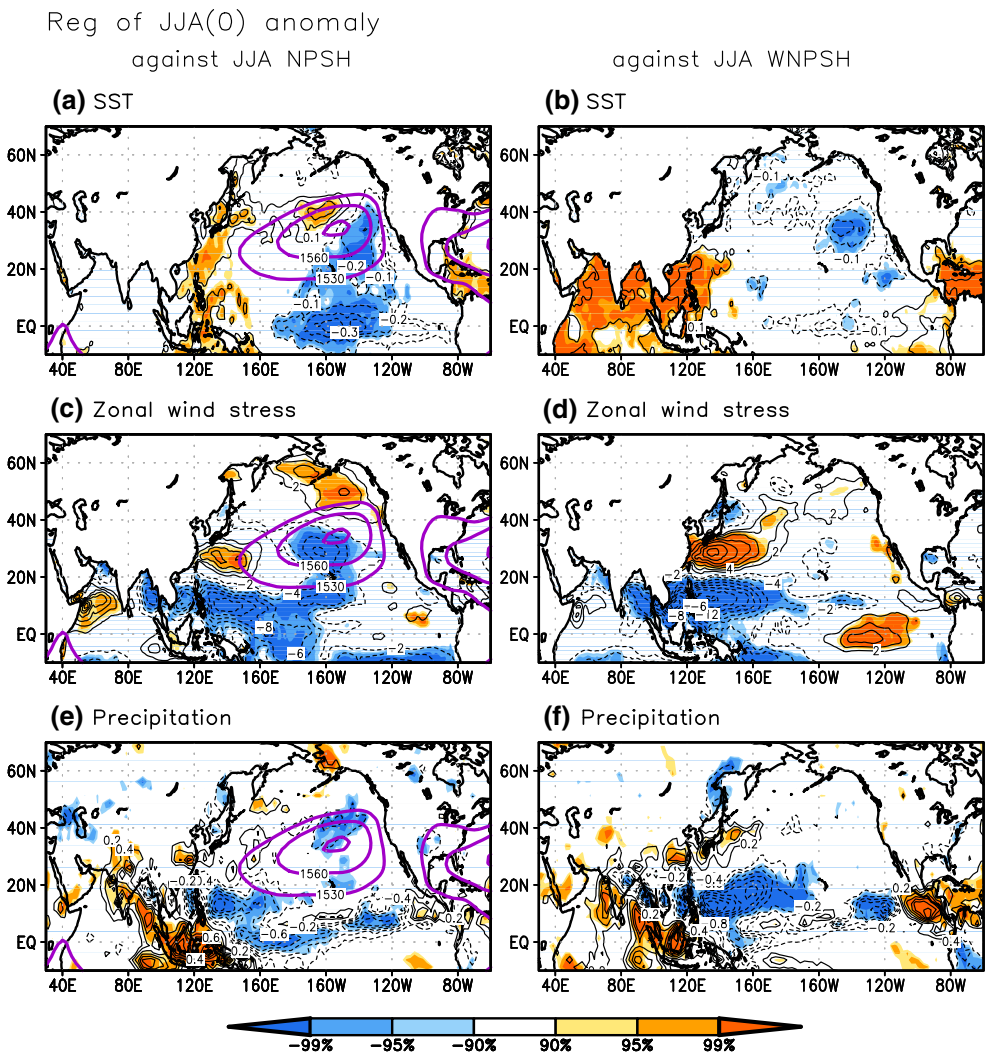

Fig. 6 **a**, **c**, and **e** Regression of JJA anomalies against JJA NPSH index. **a** SST (unit: K), **c** zonal wind stress (unit: 10^{-3} N/m^2), **e** and precipitation (mm/day). **b**, **d**, and **f** Same as **a**, **c**, and **e**, but for JJA WNPSH index. The *shading* indicates the significant anomaly above the 90 % confidence level. The *thick purple lines* in **a**, **c**, and **e** represent the geopotential height at 850 hPa greater than 1,530 gpm

ENSO decay from spring to summer, whereas the summertime NPSH accelerates the cold SST tendency during summer season. Therefore, we assert that the coupled pattern between WNPSH and NPSH is crucial for the ENSO transition from El Niño into La Niña.

How can the summer NPSH affect the ENSO transition? To understand the subtropical high-related thermal and dynamical structure, the summertime NPSH and WNPSH are regressed against the SST, zonal wind stress, and precipitation anomaly, respectively (Fig. 6). In accordance with the NPSH-related air–sea interaction (Seager et al. 2003), the SST cooling occurs on southeastern flank of the NPSH, while the SST warming appears in the northwestern flank. Interestingly, the SST cooling on the southeastern flank is extended from the subtropical North Pacific into the equatorial central Pacific. In the tropics, a strong zonal SST difference exists between the western and eastern Pacific such that warming occurs in the former and cooling occurs in the latter. The summer La Niña-like state is related to a weakened Inter-Tropical Convergence Zone (ITCZ), which is shown in Fig. 6e. Along the southern flank of the NPSH, significant easterly wind stress anomalies (i.e., stronger trade wind) are evident in tropical western and central Pacific region (160°E–160°W). The enhanced trade wind can serve as a trigger for the rapid decay of El Niño to form the QB-type ENSO.

Conversely, the WNPSH dynamics are explained by the positive thermodynamic feedback between the ocean and atmosphere (Wang et al. 2013; Kosaka et al. 2013; Xiang et al. 2013), which is significantly related to the Indian Ocean warming and western Pacific cooling anomaly (Fig. 6b). Westerly (easterly) wind stress anomalies are

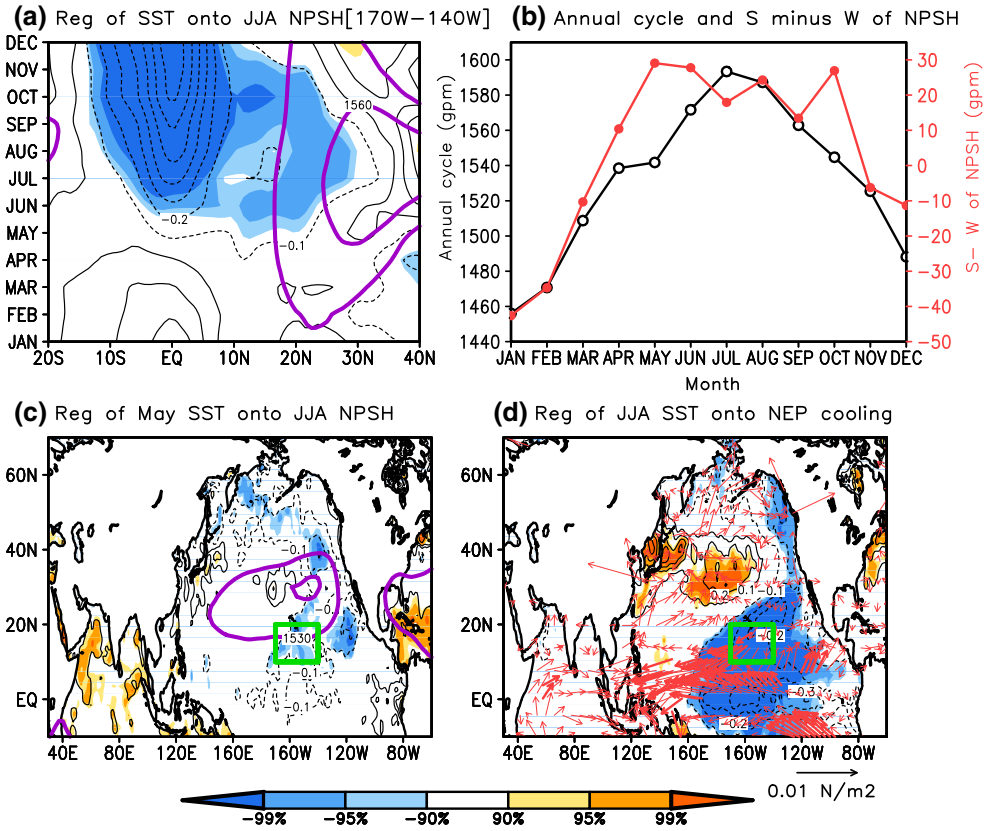

Fig. 7 **a** Latitude-time section of regression of SST anomaly averaged over the longitude 170°W–140°W against the JJA NPSH index. **b** Annual cycle of the NPSH (*black line*) and monthly difference between strong and weak NPSH years (*red line*). **c** Regression of May SST anomaly against the JJA NPSH index. **d** Regression of JJA SST (*contour*) and surface wind stress (*arrow*) against the May NEP SST cooling (denoted by *green box*). The *Purple line* in **a** and **c** indicates the climatological 1,530 and 1,560 gpm. *Shading* in **a**, **c**, **d** indicates the SST anomaly significant above the 90 % confidence level, while *thick arrow* in **d** denotes the wind stress anomaly significant above the 90 % confidence level

manifested along the northern (southern) edge of the WNPSH, and vice versa. In response of the westward exciting Rossby wave, the WNPSH is located northwest of the reduced rainfall. Overall, the enhanced rainfall over the Northern Indian Ocean and East Asian region and the suppressed rainfall over the WNP are well matched with the dynamics of the WNPSH (Wang et al. 2013; Lee et al. 2013; Xiang et al. 2013).

Figure 7a displays the persistent NPSH that occurs during the extended summer period from May to October, represented by the solid purple line. In addition to the climatological feature, the main difference in the NPSH between strong and weak NPSH years is presented in the extended summer period, indicating its prolonged effect of the NPSH (Fig. 7b). Here, strong (weak) NPSH years are defined those in which the normalized JJA-mean NPSH is greater (less) than 1.0 standard deviation: 1980, 1983, 1989, 1998, and 2010 for strong NPSH years; 1982, 1986, 1987, 1993, 2002, and 2009 for weak NPSH years. Underneath the NPSH, a significant cold SST anomaly appears after the late spring (i.e., May), and thereafter, the subtropical cold SST anomaly moves equatorward into the tropical Pacific. The May SST field regression against the JJA NPSH also shows a southwestward-tilting significant cold SST anomaly (Fig. 7c). The antecedent subtropical cooling over the northeastern Pacific [10°N–20°N, 170°W–140°W] (i.e., NEP cooling denoted in the figure by the green box) can induce the central Pacific cooling in the following summer by generating anomalous anticyclone to the west of NEP cooling and by strengthening the easterly trade wind (Fig. 7d).

Consequently, the NPSH may serve as a potential precursor to changes in tropical SST. To examine the impact of the NPSH controlling the tropical SST change, we have performed numerical experiments by using the POEM coupled model. After a 30-year continuous integration, the results from the last 20-year of the simulation were used as the control experiment (CTRL). The 20-year results of CTRL were also used to create the initial conditions for the ensemble simulation in the sensitivity experiment. The

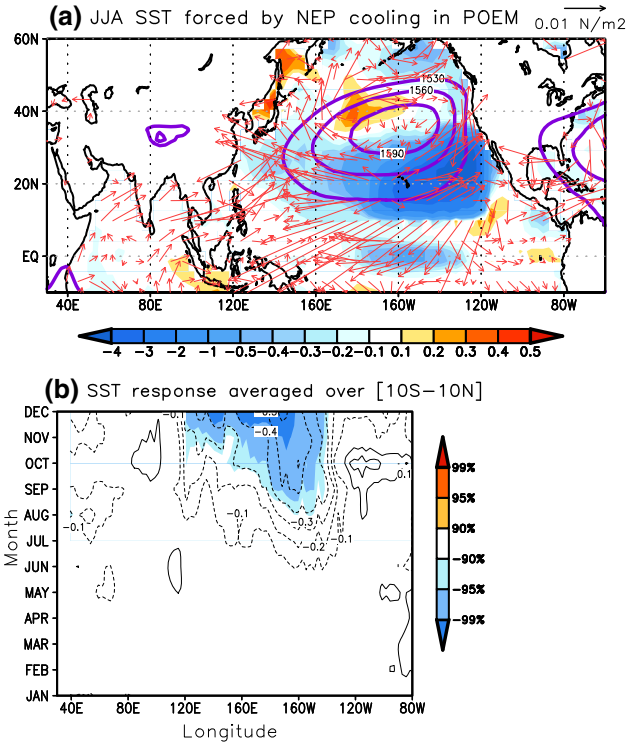

Fig. 8 **a** Difference of JJA SST (*shading*) and surface zonal wind stress (*red arrow*) between EXP_NEP minus CTRL. **b** Longitude-time section of the SST difference between EXP_NEP and CTRL averaged over the equatorial band [10°S–10°N]. EXP_NEP is performed by adding the NEP cool SST. *Shading* in **b** indicates the value significant above the 90 % confidence level

sensitivity experiment for the NEP cooling (EXP_NEP) was conducted by imposing the NPSH-related cool SST nudging in the domain [10°N–30°N, 170°W–120°W], which was obtained by doubling the JJA SST anomaly regressed against the NEP cooling, as shown in Fig. 7d. It should be noted that previous modelling studies have overlooked the influence of summer mid-latitude variability and have focused only on winter forcing (e.g., NPO during November-to-March, as reported by Vimont et al. 2009). To detect the potential influence of seasonality, the experiment was run by first adding the NEP cooling during only May-to-September (MJJAS) and also without any SST forcing during the other months (January–April and October–December). To avoid the impact of internally produced variability in the coupled model, we conducted an ensemble simulation with a 12-month integral time period (initially start at January 1 and end at December 31). A set of twenty ensemble simulations was applied in each experiment.

Figure 8a displays the JJA SST and surface wind stress response to the imposed NEP cooling. The subtropical NEP cooling induced the equatorial cooling and anomalous easterly wind over the central Pacific during JJA, which is consistent with the observed NEP cooling-related features shown in Fig. 7d. The warm SST anomaly is simulated along the northwestern flank of the NPSH. The resulting warming and NEP cooling are quite similar to the NPSH-induced SST structure shown in Fig. 6a, implying that the NEP cooling is a meaningful signal for the NPSH. As a result of the NEP SST cooling, the coupled experiment clearly shows the tropical central Pacific SST cooling. The simulated SST response exhibits a 1–2 month delay relative to the overlying NEP cooling (Fig. 8b). In particular, the extended summer SST forcing during May-to-September (MJJAS) induces central Pacific cooling after June. The cooling anomaly reaches its winter peak, which is reasonably corresponding to the ENSO transition into La Niña in observation. In summary, the coupled model results reveal that the summertime NPSH can act as a trigger for tropical central Pacific SST cooling, which supports the distinct impact of summer NPSH on the ENSO transition.

5 Discussion and conclusion

In this study, we investigated the role of summertime extratropical circulations in regulating the rapid ENSO transition from El Niño to La Niña. To achieve this, the difference between QB and LF-type ENSO was examined by using two methodologies including the filtering of QB and LF periods and composite analysis of QB- and LF-type ENSO years. In the two methodologies, the main difference in extratropical circulation between QB- and LF-type ENSO is characterized by the polarity of variability for WNPSH and NPSH during the summer season. The QB-type ENSO shows an in-phase relationship between WNPSH and NPSH manifested by strengthening of the two systems, whereas the LF-type ENSO exhibits an out-of-phase relationship between the two high systems (i.e., enhanced WNPSH but weakened NPSH). Actually, several QB-type ENSO years including 1972/1973, 1982/1983, and 1997/1998 are associated with the strong El Niño turnabout. Previous researches have reported that the anomalous WNPSH plays an important role in initializing the termination of the strong El Niño (Wang and Li 2004; Liu and Xue 2010a). The stronger El Niño during the preceding winter leads to the more strengthened WNPSH from spring to summer, which it thereby is responsible for the initial decay of El Niño via modulation of the easterly wind in the western Pacific.

On the contrary, the NPSH has a stronger connection with the decaying El Niño process after the boreal summer, which provides a possible mechanism for the rapid decay of El Niño to form a QB-type ENSO. The NPSH variability might be more affected by the temporal evolution of El

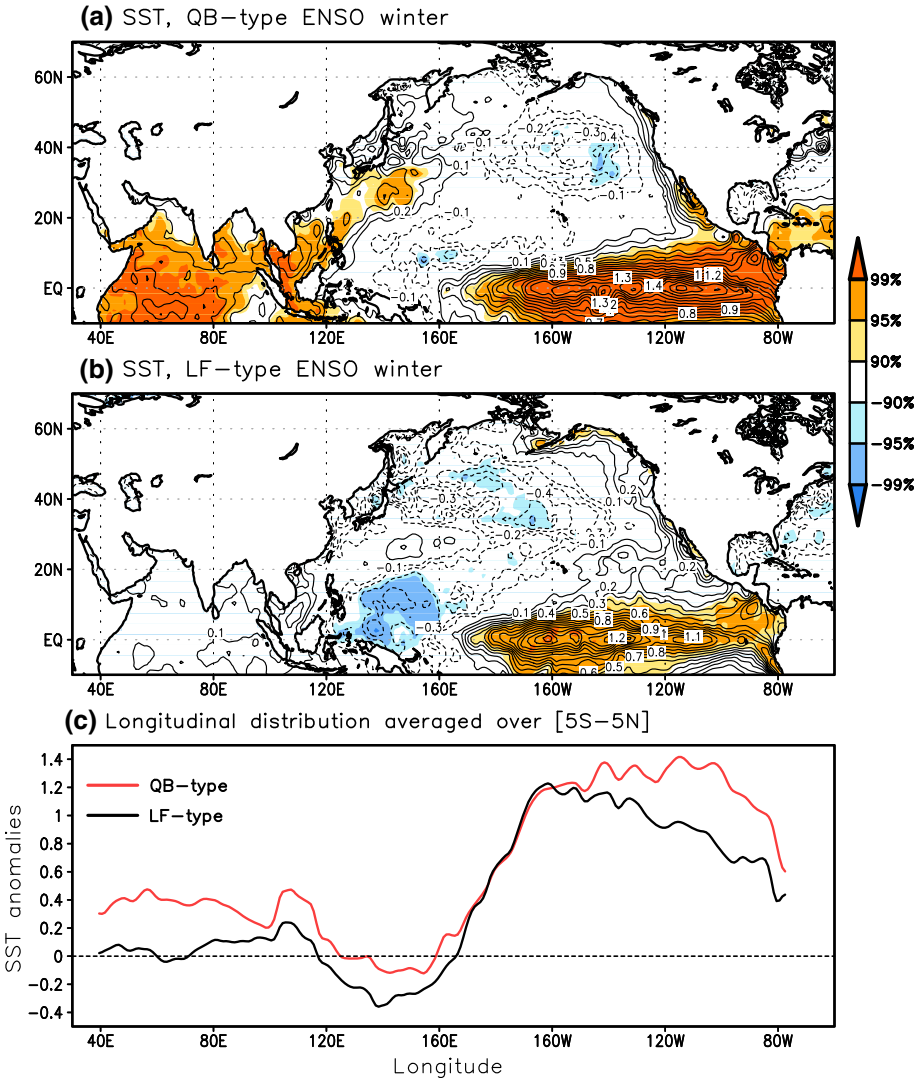

Fig. 9 SST anomaly for the **a** QB- and **b** LF-type ENSO winters during 1958–2010. **c** Longitudinal distribution of the SST anomalies for the QB- and LF-type ENSO winters averaged over [5°S–5°N]. *Shading* in **a**–**b** indicates the value significant above 90 % confidence level

Niño than by the magnitude of El Niño in the preceding winter. Recently, Yun et al. (2013) have demonstrated that the Indian Ocean SST warming after the El Niño winter triggers an abrupt decaying El Niño (Kug and Kang 2006; Chen et al. 2012), and consequently, leads to the coexistence of the Indian Ocean-western Pacific warming and eastern Pacific cooling and resultant enhancement of summer coupled pattern of NPSH and WNPSH via the atmosphere bride. Meanwhile, the western Pacific SST cooling after the El Niño winter tends to generate the summer dipole SST structure between western Pacific cooling and eastern Pacific warming, which it interrupts the development of the NPSH. A warmer Indian Ocean SST occurs in the QB-type ENSO winter, whereas a cooler western Pacific SST appears in the LF-type ENSO winter (see Figs. 2a, b, 9). The different temporal evolutions between QB- and LF-type ENSO also corresponds well to those shown in Yun et al. (2013). Consequently, the SST evolutions after the QB-type ENSO winter may provide a more favorable condition for developing the NPSH than those after the LF-type ENSO winter.

As a prolonged extratropical circulation occurring during the boreal summer, the NPSH causes a late spring subtropical cooling over the northeastern Pacific, which is accompanied by an anomalous anticyclone west of the cooling center. This cold SST anomaly tends to migrate equatorward through the wind-evaporation-SST feedback, and thus results in an enhanced easterly trade wind south of the anticyclone. Finally, the strengthening of the trade wind could lead to the early decay of the El Niño event during the boreal summer. In addition, the coupled model experiments demonstrated that the summer NPSH can play an important role in generating the tropical central Pacific SST cooling, which supports the assertion that summer NPSH contributes to the rapid ENSO transition. However, it cannot be excluded that the central Pacific cooling can

favor the NPSH with some positive feedbacks to sustain the NPSH. This feedback process between the NPSH and central Pacific SST could maintain the NPSH itself for 5 months or even longer, which will be examined in future research.

It was previously reported that the WNPSH itself has two distinctive periodicities with QB and LF (Sui et al. 2007), while the NPSH exhibits dominant QB periodicity (Yu et al. 2010). The previous findings reasonably correspond to those shown in the present study. Despite the remarkable LF variability of WNPSH, the earlier studies have focused mainly on the QB-like oscillation between WNPSH and ENSO (e.g., Chang et al. 2000; Li et al. 2007). We conclude that the QB-type ENSO is significantly connected with the coupled WNPSH–NPSH pattern, which may be a coupled process between the tropics and midlatitudes. The coupled feature between ENSO and extratropical subtropical highs would lead to the QB-like correlation between EASM and ENSO (Shen and Lau, 1995), as well. On the other hand, this observation study cannot fully explain the relative contribution of the WNPSH and NPSH on ENSO transition, which should be examined in the numerical experiments using CGCM in a future work.

Several issues remain elusive and call for the further study. McGregor et al. (2012) have demonstrated that the southward shift of the equatorial wind is important for the ENSO transition. In addition, Liu and Xue (2010b) have shown that the decaying process of a moderate El Niño is related to variability in the South Pacific subtropical high. The possible impact of these factors on the ENSO transition should be investigated in further study. The NPSH-related tropical SST cooling resembles the central Pacific (CP)-type ENSO. Recent studies have reported that the CP-type ENSO events have become more frequent and more intense since the early 1990s (e.g., Yeh et al. 2009; Lee and McPhaden 2010). This hints decadal changes in relationship between the subtropical highs and ENSO, which will be investigated in the following study.

The SST pattern of the QB-type ENSO winter shows the maximum warming in the eastern Pacific (EP), while that of the LF-type ENSO winter exhibits the maximum in the CP (see Figs 2a, b, 9a, b). Accordingly, a warmer EP SST tends to occur in the QB-type ENSO winter compared to LF-type ENSO (Fig. 9c), implying an association between the temporal (QB/LF-type) and spatial (EP/CP-type) characteristics of ENSO. The mechanisms for EP-type ENSO rely heavily on thermocline feedbacks as a delayed oscillator, while those for CP-type ENSO is modulated by the zonal advection of mean SST by the anomalous zonal current (Suarez and Schopf 1988; Kug et al. 2009) and is further influenced by extratropical atmospheric forcing (Yu et al. 2010). Recently, Lopez and Kirtman (2013) have argued that westerly wind bursts enhance the thermocline mechanism as opposed to the zonal advection mechanism, hence a stronger response for the EP-type ENSO, which favors the following CP-type events. The possible connection between the temporal and spatial characteristics of ENSO is the subject of some debate (Ha et al. 2012) and will be investigated in the future study. The process may be driven by the oscillatory tendency of the tropical Pacific ocean–atmosphere coupled system, which involves TBO dynamics. The present study may contribute to an understanding of the coupled system between the tropics and midlatitudes and to improvement in ENSO prediction.

Acknowledgments This study was financially supported by GRL grant of the National Research Foundation (NRF) funded by the Korean Government (MEST 2011-0021927). B. Xiang was partly supported by NOAA MAPP Program under Awards NA12OAR4310075. S.-W. Yeh is supported by the Brain Korea 21 Plus Project in Department of Marine Sciences and Convergent Technology of Hanyang University.

References

Adler RF, Huffman GJ, Chang A et al (2003) The version 2 global precipitation climatology project (GPCP) monthly precipitation analysis (1979-Present). J Hydrometeor 4:1147–1167

Barnett TP (1991) The interaction of multiple time scales in the tropical climate system. J Clim 4:269–285

Bejarano L, Jin FF (2008) Coexistence of equatorial coupled modes of ENSO. J Clim 21:3051–3067

Carton JA, Giese BS (2008) A reanalysis of ocean climate using simple ocean data assimilation (SODA). Mon Wea Rev 136:2999–3017

Chang CP, Zhang Y, Li T (2000) Interannual and interdecadal variations of the East Asian summer monsoon and tropical Pacific SSTs. Part I: roles of the subtropical ridge. J Clim 13:4310–4325

Chen W, Park J-K, Dong B, Lu R, Jung W-S (2012) The relationship between El Niño and the western North Pacific summer climate in a coupled GCM: role of the transition of El Niño decaying phases. J Geophys Res 117:D12111. doi:10.1029/2011JD017385

Danabasoglu G, Large WG, Tribbia JJ, Gent PR, Briegleb BP, McWilliams JC (2006) Diurnal coupling in the tropical oceans of CCSM3. J Clim 19:2347–2365

Ha K-J, Yoon S-J, Yun K-Y, Kug J-S, Jang Y-S, Chan JCL (2012) Dependency of typhoon intensity and genesis locations on El Niño phase and SST shift over the western North Pacific. Theor Appl Climatol 109:383–395

Kalnay E et al (1996) The NCEP/NCAR 40-year reanalysis project. Bull Am Meteorol Soc 77:437–471

Kanamitsu M, Ebisuzaki W, Woollen J, Yang SK, Hnilo JJ, Fiorino M, Potter GL (2002) NCEP-DOE AMIP-II reanalysis (R-2). Bull Am Meteorol Soc 83:1631–1643

Kim K-Y, Kim Y-Y (2002) Mechanism of Kelvin and Rossby waves during ENSO events. Meteorol Atmos Phys 81:169–189

Kim K-M, Lau K-M (2001) Dynamics of monsoon-induced biennial variability in ENSO. Geophys Res Lett 28(2):315–318

Kosaka Y, Xie S-P, Lau N-C, Vecchi GA (2013) Origin of seasonal predictability for summer climate over the Northwestern Pacific. Proc Natl Acad Sci USA 110(19):7574–7579

Kug J-S, Kang I-S (2006) Interactive feedback between ENSO and the Indian Ocean. J Clim 19:1784–1801

Kug J-S, Jin F-F, An S-I (2009) Two types of El Niño events: cold tongue El Niño and warm pool El Niño. J Clim 22:1499–1515

Lau K-M, Lee J-Y, Kim K-M, Kang I-S (2004) The north Pacific as a regulator of summertime climate over Eurasia and North America. J Clim 17:819–833

Lee T, McPhaden MJ (2010) Increasing intensity of El Niño in the central-equatorial Pacific. Geophys Res Lett 37:L14603. doi:10.1029/2010GL044007

Lee S-S, Seo Y-W, Ha K-J, Jhun J-G (2013) Impact of the western North Pacific subtropical high on the East Asian monsoon precipitation and the Indian Ocean precipitation in the boreal summertime. Asia-Pac J Atmos Sci 49(2):171–182

Li T, Zhang Y (2002) Processes that determine the quasi-biennial and lower-frequency variability of the South Asian monsoon. J Meteor Soc Japan 80(5):1149–1163

Li Y, Lu R, Dong B (2007) The ENSO-Asian monsoon interaction in a coupled Ocean–Atmosphere GCM. J Clim 20:5164–5177

Liu C-Z, Xue F (2010a) The Decay of El Niño with different intensity. Part I, the decay of the strong El Niño. Chin J Geophys 53:14–25

Liu C-Z, Xue F (2010b) The Decay of El Niño with different intensity. Part II, the decay of the moderate and relatively-weak El Niño. Chin J Geophys 53:915–925

Liu Z, Yang H (2003) Extratropical control of tropical climate, the atmospheric bridge and oceanic tunnel. Geophys Res Lett 30(5):1230. doi:10.1029/2002GL016492

Lopez H, Kirtman BP (2013) Westerly wind bursts and the diversity of ENSO in CCSM3 and CCSM4. Geophys Res Lett 40:4722–4727. doi:10.1002/grl.50913

McGregor S, Timmermann A, Schneider N, Studecker MF, England MH (2012) The effect of the South Pacific convergence zone on the termination of El Nino events and the meridional asymmetry of ENSO. J Clim 25:5566–5586

Meehl GA (1997) The South Asian monsoon and the tropospheric biennial oscillation. J Clim 10:1921–1943

Rayner NA et al (2003) Global analyses of sea surface temperature, sea ice, and night marine air temperature since the late nineteenth century. J Geophys Res 108(D14):4407. doi:10.1029/2002JD002670

Rodwell M, Hoskins BJ (2001) Subtropical anticyclones and summer monsoons. J Clim 14:3192–3211

Roeckner E et al (1996) The atmospheric general circulation model ECHAM-4: model description and simulation of present-day climate. Max Planck Institute for Meteorology Rep 218: 90 pp

Seager R, Murtugudde R, Raik N, Clement A, Gordon N, Miller J (2003) Air-sea interaction and the seasonal cycle of the subtropical anticyclones. J Clim 16:1948–1966

Shen S, Lau K-M (1995) Biennial oscillation associated with the East Asian summer monsoon and tropical sea surface temperature. J Meteor Soc Japan 73:105–124

Smith RD, Dukowicz JK, Malone RC (1992) Parallel ocean general circulation modeling. Physica D 60:38–61

Suarez MJ, Schopf PS (1988) A delayed action oscillator for ENSO. J Atmos Sci 45:3283–3287

Sui C-H, Chung P-H, Li T (2007) Interannual and interdecadal variability of the summertime western North Pacific subtropical high. Geophys Res Lett 34:L11701. doi:10.1029/2006GL029204

Valcke S, Terray L, Piacentini A (2000) OASIS 2.4 Ocean atmospheric sea ice soil user's guide, Version 2.4. CERFACS Tech Rep CERFACS TR/CMGC/00-10: 85 pp

Vimont DJ, Wallace JM, Battisti DS (2003) The seasonal footprinting mechanism in the Pacific: implications for ENSO. J Clim 16:2668–2675

Vimont DJ, Alexander M, Fontaine A (2009) Midlatitude excitation of tropical variability in the Pacific: the role of thermodynamic coupling and seasonality. J Clim 22:518–534

Wang B, An S-I (2005) A method for detecting season-dependent modes of climate variability: S-EOF analysis. Geophys Res Lett 32:L15710. doi:10.1029/2005GL022709

Wang B, Li T (2004) East Asian monsoon-ENSO interactions. In: Chang C-P (ed) East Asian monsoon. World Scientific, Singapore, pp 177–212

Wang B, Wu R, Lukas R (1999) Roles of the western North Pacific wind variation in thermocline adjustment and ENSO phase transition. J Meteor Soc Japan 77:1–16

Wang B, Wu R, Fu X (2000) Pacific-East Asia teleconnection: how does ENSO affect East Asian climate? J Clim 13:1517–1536

Wang B, Xiang B, Lee J-Y (2013) Subtropical high predictability establishes a promising way for monsoon and tropical storm predictions. Proc Natl Acad Sci USA 110(8):2718–2722

Weisberg RH, Wang C (1997) A western Pacific oscillator paradigm for the El Niño-Southern Oscillation. Geophys Res Lett 24(7):779–782

Wu R, Kirtman BP (2004) The tropospheric biennial oscillation of the monsoon—ENSO system in an interactive ensemble coupled GCM. J Clim 17:1623–1640

Xiang B, Wang B, Ding Q, Jin F-F, Fu X, Kim H-J (2012) Reduction of the thermocline feedback associated with mean SST bias in ENSO simulation. Clim Dyn 39:1413–1430. doi:10.1007/s00382-011-1164-4

Xiang B, Wang B, Yu W, Xu S (2013) How can anomalous western North Pacific subtropical high intensify in late summer? Geophys Res Lett 40(10):2349–2354. doi:10.1002/grl.50431

Yasunari T (1990) Impact of Indian monsoon on the coupled atmosphere/ocean system in the tropical Pacific. Meteorol Atmos Phys 44:29–41

Yeh S-W, Kug J-S, Dewitte B, Kwon M-H, Kirtman B, Jin F-F (2009) El Niño in a changing climate. Nature 461:511–514. doi:10.1038/nature08316

Yu J-Y, Kim S-T (2011) Relationships between extratropical sea level pressure variations and the central Pacific and eastern Pacific types of ENSO. J Clim 24:708–720

Yu J-Y, Kao H-Y, Lee T (2010) Subtropics-related interannual sea surface temperature variability in the equatorial central Pacific. J Clim 23:2869–2884

Yun K-S, Ren B, Ha K-J, Chan JCL, Jhun J-G (2009) The 30–60-day oscillation in the East Asian summer monsoon and its time-dependent association with the ENSO. Tellus 61A:565–578

Yun K-S, Kim S-Y, Ha K-J, Watanabe M (2011) Effects of subseasonal basic state changes on Rossby wave propagation during northern summer. J Geophys Res 116:D24102. doi:10.1029/2011JD016258

Yun K-S, Yeh S-W, Ha K-J (2013) Distinct impacts of tropical SSTs on summer North Pacific high and western North Pacific subtropical high. J Geophys Res 118:4107–4116. doi:10.1002/jgrd.50253